Accelerated Reactivity Mechanism and Interpretable Machine Learning Model of *N*-Sulfonylimines Towards Fast Multicomponent Reactions

Krupal P. Jethava,‡ Jonathan Fine,‡ Yingqi Chen, Ahad Hossain, Gaurav Chopra[1,2] *

[1]Department of Chemistry, Purdue University, West Lafayette, IN 47907, USA. [2]Purdue Institute for Drug Discovery, Purdue Institute for Integrative Neuroscience, Purdue Institute for Inflammation, Immunology and Infectious Disease, Purdue Center for Cancer Research, Purdue University, Integrative Data Science Initiative, West Lafayette, IN 47907, USA

ABSTRACT: Predicting the outcome of chemical reactions using machine learning models has emerged as a promising research area in chemical science. However, the use of such models to prospectively test new reactions by interpreting chemical reactivity is limited. We have developed a new fast and one-pot multicomponent reaction of *N*-sulfonylimines with heterogenous reactivity. Fast reaction times (<5 min) for both acyclic and cyclic sulfonylimine encouraged us to investigate plausible reaction mechanisms using quantum mechanics to identify intermediates and transition states. The heterogeneous reactivity of *N*-sulfonylimine lead us to develop a human-interpretable machine learning model using positive and negative reaction profiles. We introduce chemical reactivity flowcharts to help chemists interpret the decisions made by the machine learning model for understanding heterogeneous reactivity of *N*-sulfonylimines. The model learns chemical patterns to accurately predict the reactivity of *N*-sulfonylimine with different carboxylic acids and can be used to suggest new reactions to elucidate the substrate scope of the reaction. We believe our human-interpretable machine learning approach is a general strategy that is useful to understand chemical reactivity of components for any multicomponent reaction to enhance synthesis of drug-like libraries.

1. INTRODUCTION

Computer-assisted organic chemistry has a huge potential for predicting chemical reaction conditions and for automating synthetic chemistry.[1,2,3] In recent years, machine learning (ML) based approaches have been successfully applied to screen libraries of druglike molecules,[4,5] for quantitative structure-activity relationships (QSAR),[6] for retrosynthetic planning[7], and for reaction condition prediction. Reactivity prediction is a hard problem that often require specific experimental datasets to train ML models.[8,9] Traditionally, creating such experimental databases requires a large number of manual experiments to check the feasibility of available starting materials to react together. However, with careful training of ML models using both positive and negative reaction data, it is possible to train on smaller datasets to test specific synthetic objectives. The results from ML models are helpful in building a chemical library that is otherwise tedious to explore by screening each reaction to check substrate feasibility under certain reaction conditions. To date, there is limited literature precedence for prospective prediction of desired chemical reactions and interpreting its reactivity using machine learning methods.[10,11] We provide a first report, to the best of our knowledge, of a fast and one-pot multicomponent reaction to explore heterogenous reactivity of *N*-sulfonylimines by training a human-interpretable machine learning model that identifies chemical patterns of reactivity to predict and test new reactions prospectively.

We selected *N*-sulfonylimines as our model substrate because *N*-sulfonylimines are one of the important synthons in organic chemistry that are being used for a variety of chemical transformations. *N*-sulfonylimine is a good source of an electrophilic carbon for radical[12] and nucleophilic addition[13] reactions. There are several reports available for *N*-sulfonylimines reactions where a carbon-nitrogen double bond is exploited.[14] Notably, the use sulfamidate[15], a cyclic *N*-sulfonylimine, has been used to prepare interesting heterocyclic scaffolds. Sulfamidate is transformed into a fused heterocycle using a Michael addition[16], cycloaddition[17–22], arylation[23–25], alkenylation[26–28], or alkynylation[26] strategy by leveraging electrophilicity of cyclic *N*-sulfonylimines (**Scheme 1**).

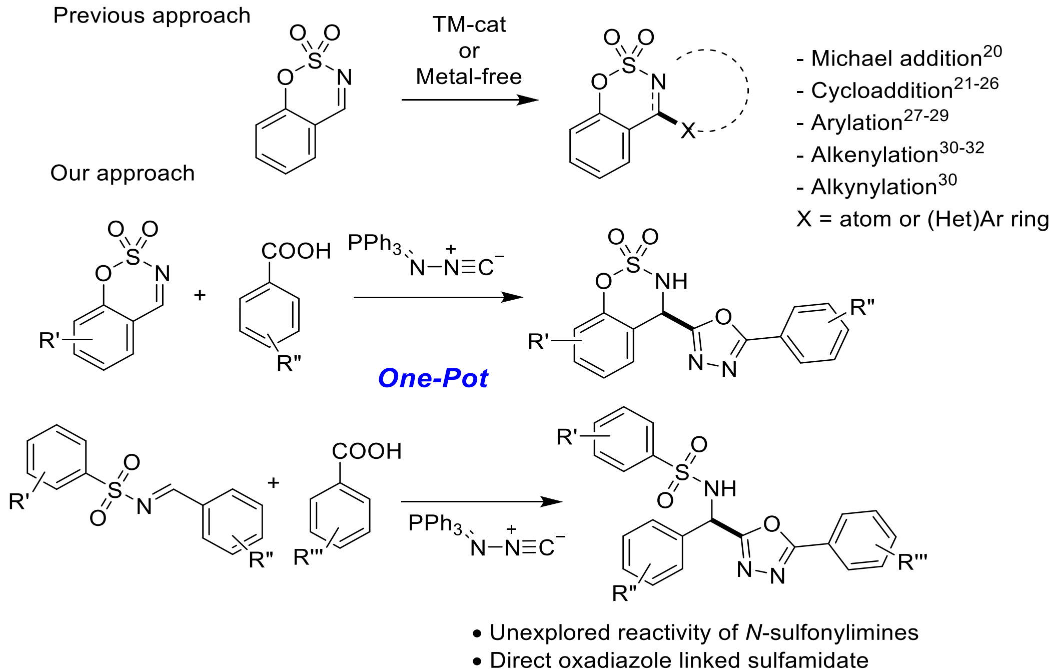

Scheme 1: Strategy to explore *N*-sulfonylimine reactivity towards multicomponent reaction

However, among reported synthetic strategies, construction of direct C-C bond between the imine carbon and the (het)aromatic partner is underrepresented in the literature. Specifically, a synthetic strategy for the direct C-C bond linkage between sulfamidate and oxadiazole has not been explored till date. The oxadiazole scaffold finds a unique presence in many biologically active compounds,[29,30] pharmaceutical agents, and is a privileged scaffold in material science.[31] Among different types of five-membered heterocycles, 1,3,4-oxadiazole plays an important role in organic synthesis and medicinal chemistry representing broad spectrum bioactivity as anticancer, antimicrobial, antiviral, and antifungal pharmacological agents[32,33] (**Figure 1**). For example, the recently discovered CA-170 contains a 1,3,4-oxadiazole moiety and is a promising immune checkpoint inhibitor in the tumor microenvironment as a dual antagonist of Programmable death ligand-1 and V-domain Ig suppressor of T-cell activation. Although the structure of CA-170 is not disclosed, a speculated structure is shown in **Figure 1**.[34] Conventional approaches to synthesize 1,3,4-oxadiazole is a multistep procedure that includes transformation of carboxylic acid into acyl chloride. Then a nucleophilic substitution reaction with hydrazide to produce an amide bond followed by cyclization step to get a 1,3,4-oxadiazole.[35]

Multicomponent reactions (MCRs) have attracted medicinal chemists to prepare chemical libraries of biologically important molecules and drugs[36] using two or more building blocks, often in reduced synthetic steps or one-pot experimental settings.[37,38,39,40] These building blocks are either commercially available or easily synthesizable in the lab. Importantly, MCRs are extremely useful in diversity-oriented drug discovery to prepare diverse chemical libraries in a short time scale compare to traditional synthesis using sequential reactions. But, MCR is highly dependent on the nature of the solvents, catalysts, concentrations and equivalent of reagents being used.[36] Once a set of parameters have been defined, a specific MCR can be used in combinatorial chemistry as well as synthesis by automation. However, it does not warrant the formation of desire products due to the variable reactivity of starting materials. The understanding of chemical reactivity of starting materials for a particular MCR would be useful to identify which starting materials to use. This important information of chemical reactivity can used to make a machine learning model which can suggest a type of starting materials to be used to get desire product successfully which would also reduce the waste of valuable reagents, time and efforts. Keeping this in mind, we selected a model MCR using *N*-sulfonylimine and carboxylic acid containing starting materials by taking inspiration from the previously reported MCR *albeit* using different reactants. Ramazani et al.[41] reported a four-component reaction yielding 1,3,4-oxadiazole scaffold using aromatic aldehyde, benzoic acid, *N*-isocyano triphenylphosphorane (PINC), and secondary amine as reaction partners. The formation of 1,3,4-oxadiazole involves an essential reactant, PINC which is the nucleophilic partner that reacts with the imine. This species is generated *in situ* from the amine and aldehyde and reacts with a carboxylic acid followed by cyclization to yield 1,3,4-oxadiazole. A similar strategy was extended by Yudin et al.[42,43] to perform an intramolecular reaction for the synthesis of oxadiazole containing cyclic peptide or macrocycle where two end terminals are stapled to form oxadiazole ring. This strategy also relies upon *in situ* imine formation from an aldehyde, a secondary amine, and additional amine group. It is noteworthy that *in situ* formations of imines are not always favorable as it is highly dependent upon its starting materials – an aldehyde and an amine, potentially limiting the use of these approaches. To address this issue, we provide the first report to use *N*-sulfonylimine as a substrate for a fast and single-step approach to synthesize sulfamidate embedded 1,3,4-oxadiazole using a MCR.

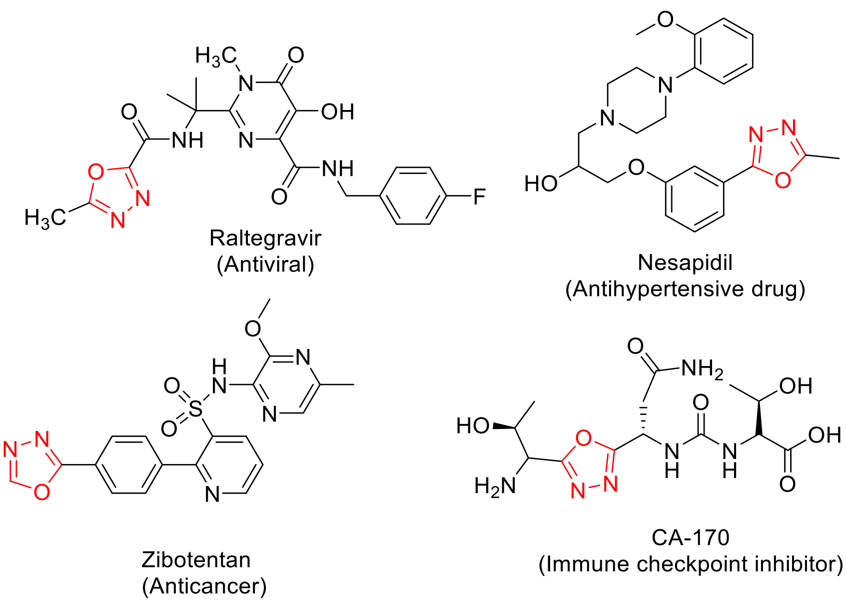

Figure 1. Showing compounds with presence of 1,3,4-oxadiazole in medicinal chemistry.

We started our investigation with the idea that several types of cyclic *N*-sulfonylimines (aldimines or ketimines), acyclic *N*-sulfonylimines, and aromatic imines can be synthesized. To determine the reactivity pattern of various imines with carboxylic acids, we used Fukui reaction parameters calculated using Density Functional Theory (DFT)[44] and identified the most suitable imines using the electrophilicity of the carbon atom (**Figure S1**). Both cyclic and acyclic *N*-sulfonylimines are highly susceptible toward nucleophilic attack of carboxylic acids. Therefore, we started using the model substrate cyclic *N*-sulfonylimine (sulfamidate) **1a,** which can be easily synthesized from substituted salicylaldehydes. We initially selected benzoic acid as the reaction partner because of its moderate nucleophilic tendency (**Figure S1**) and the selection of optimized conditions for future use with a chemically diverse range of carboxylic acids. Further, the synthesis of other derivatives with the optimized condition would serve as a training dataset to develop a machine learning model.

2. RESULTS AND DISCUSSION

2.1. Reaction Development and Optimization

Having a synthetic and computational strategy in mind, we performed an optimization study using sulfamidate (**1a**) and benzoic acid (**2a**) to form the desired product **3a**. Reaction conditions from the literature for similar MCRs resulted in a messy TLC and trace product formation as identified using HPLC-MS (entry 1 in **Table 1**). The replacement of a mixture of solvents with only dichloroethane (DCE) and room temperature conditions gave trace amounts of product as detected by HPLC-MS (entry 2). Next, replacing dichloroethane with dichloromethane (DCM) afforded a detectable quantity of desired product **3a** (entry 3). While doing a time-point study with a 30 minutes interval, we observed that the desired product was formed within 30 minutes (entry 4). However, TLC analysis shows multiple products, so we decreased the reaction temperature. At 0°C the desired product formed within 5 minutes (entry 5) as determined by a 5 minute time-point study. In all the above attempts, benzoic acid was added slowly. At -10°C, an additional experiment where DCM is added at the end increased the yield significantly (entry 6 vs 7) - suggesting that sulfamidate has high reactivity.

Table 1. Optimization of the synthesis of 1,3,4-oxadiazole[a]

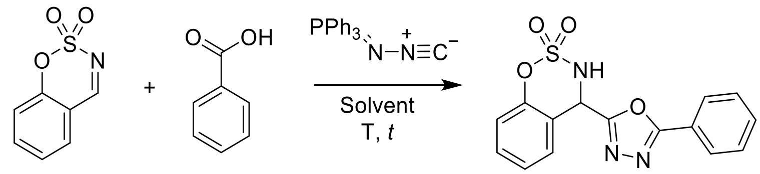

1a **2a** **3a**

Entry	Solvent(s)	T (°C)	*t* (min)	Yield (%)[e]
1[b]	DCE:MeCN	50	120	Trace
2	DCE	25	120	Trace
3	DCM	25	120	<5
4	DCM	25	30 to 120	<5
5	DCM	Ice-bath	5 to 30	25
6[c]	DCM	-10	5	40
7[d]	DCM	-10	5	67

[a] Reactions are at 0.1 mmol scale; [b] Reaction condition followed as per literature[42]; [c] benzoic acid added at the end; [d] all solid components were taken together and solvent added at the end; [e] isolated yield; T = Temperature and *t* = time

Next, we applied the optimized reaction condition to the acyclic imine selected using DFT calculations (**Figure S1**) as it was the second most reactive imine. Interestingly, the reaction afforded the desired product with good yield (**Scheme 2**), but with longer reaction time (10 mins) for the complete conversion as compared to sulfamidate (<5 min). This led us to investigate the mechanism and the energy profile of various plausible intermediates formed in this reaction.

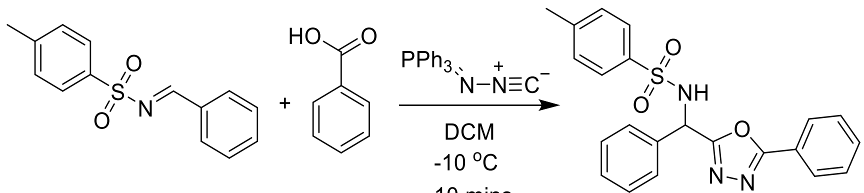

4a **2a** **5a** (78%)

Scheme 2. Synthesis of 1,3,4-oxadiazole using acyclic imine with benzoic acid with optimized reaction conditions.

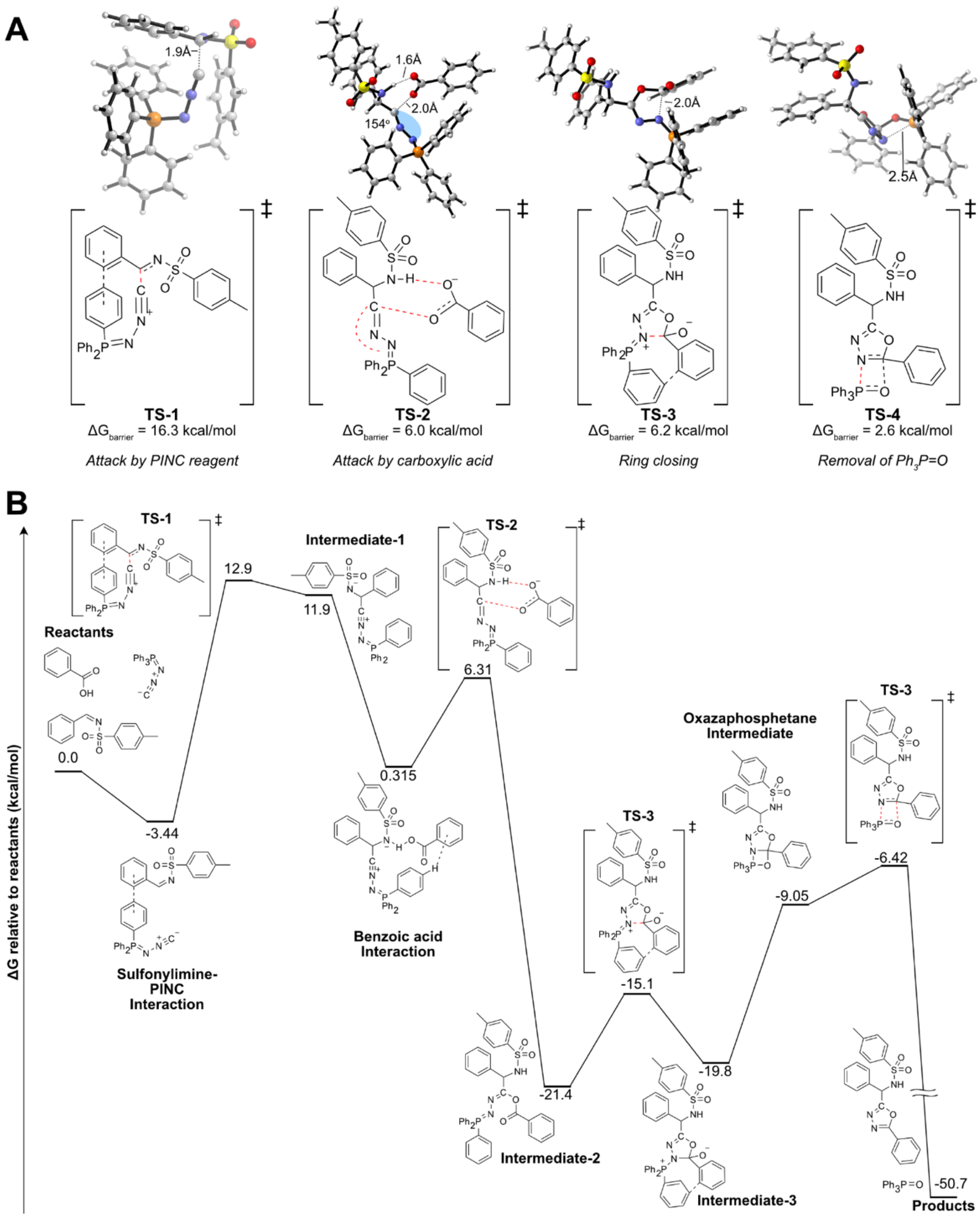

Figure 2. Calculated transition states, intermediates and energy profiles for acyclic *N*-sulfonylimines. **A.** 3D and 2D structure of each transition states for the acyclic reaction with their respective geometries and interaction (show in red in 2D). **B.** DFT optimized reaction mechanism with energies shown with respect to the reactants. All calculations were performed using a polarized continuum model for DCM solvation at -10°C. The largest energy barrier of 16.3 kcal/mol is between the acyclic sulfonylimine/PINC interaction complex and the first transition state (TS-1). The reaction is predicted to be highly exergonic with ΔG= –50.7 kcal/mol. PINC = *N*-isocyano triphenylphosphorane, $Ph_3P=O$ is triphenylphosphine oxide, TS = Transition State. Color code: grey, carbon; red, oxygen; blue, nitrogen; orange, phosphorous; yellow, sulphur; white, hydrogen. Full coordinates and animations can be found at https://chopralab.github.io/n_sulfonylimine_reactions.

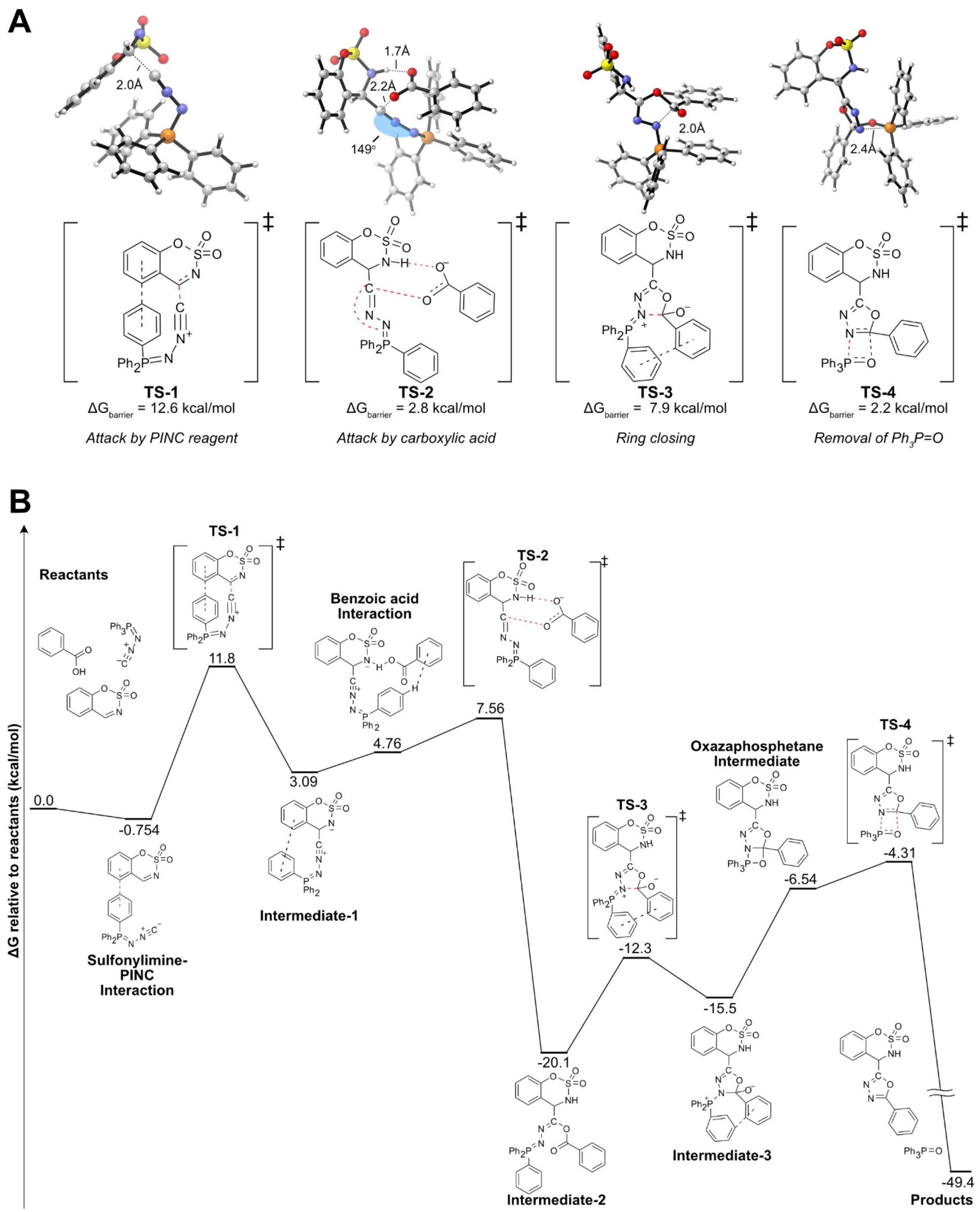

Figure 3. Calculated transition states, intermediates and energy profiles for cyclic *N*-sulfonylimines. A. 3D and 2D structure of each transition states for the acyclic reaction with their respective geometries and interaction (show in red in 2D). These geometries are similar to ones obtained for the acyclic reaction. **B.** DFT optimized reaction mechanism with energies shown with respect to the reactants. All calculations were performed using a polarized continuum model for DCM solvation at -10°C. The rate limiting step has a barrier energy of 12.6 kcal/mol between the cyclic sulfonylimine/PINC interaction complex and the first transition state (TS-1). The reaction is predicted to be highly exergonic with ΔG= –49.4 kcal/mol. PINC = *N*-isocyano triphenylphosphorane, $Ph_3P{=}O$ is triphenylphosphine oxide, TS = Transition State. Color code: grey, carbon; red, oxygen; blue, nitrogen; orange, phosphorous; yellow, sulphur; white, hydrogen. Full coordinates and animations can be found at https://chopralab.github.io/n_sulfonylimine_reactions.

2.2. DFT calculations for reaction mechanism

To gain mechanistic insights of the chemical reactions, we conducted DFT calculations using a polarized continuum model for DCM solvation at –10 °C to identify transition states and intermediates for acyclic and cyclic *N*-sulfonylimines (**Figures 2**, **3**). The nucleophilic attack by negatively charged carbon atom of PINC on the electrophilic center of *N*-sulfonylimine yields Intermediate-1. The subsequent Intermediate-2 is formed by a nucleophilic attack of benzoic acid. Next, intramolecular cyclization at the carbonyl carbon and subsequent removal of triphenylphosphine oxide yields the desired 1,3,4-oxadiazole containing the product. Both imines have the same rate-limiting step where the PINC reagent attacks the carbonyl carbon and both steps have small activation energies (12.6 kcal/mol and 16.3 kcal/mol for the cyclic and acyclic imines respectively), suggesting both reactions will occur quickly (see **Supporting text for reaction mechanism section** for a detailed description).

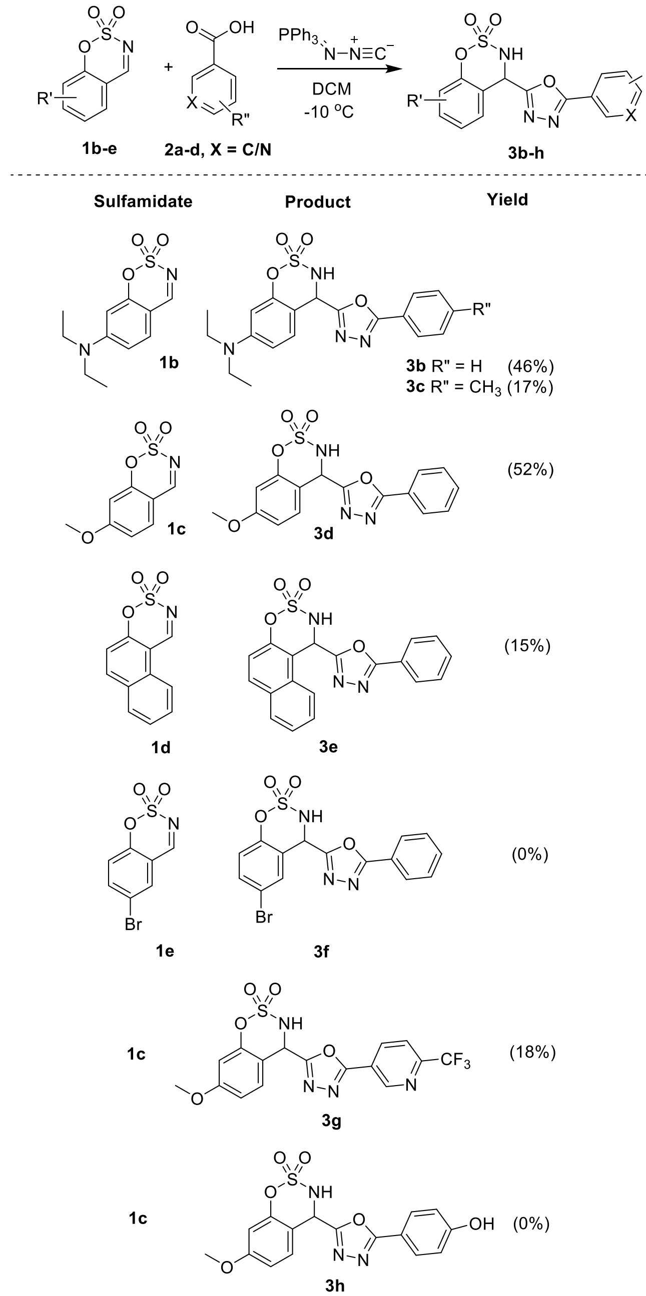

Scheme 3. Substrate scope for representative cyclic *N*-sulfonyl-imine with various carboxylic acids used as training data.

2.3. Investigating reactivity of cylic and acyclic *N*-sulfonylimines

Using the optimized conditions, we started investigating various sulfamidates and carboxylic acid derivatives. The reaction of the diethylamine containing sulfamidate (**1b**) with benzoic acid afforded desired product **3b** in 46% yield. The reaction of sulfamidate **1b** with *p*-toluic acid (**2b**) also formed product **3c** but in low yield (17%). Further, reaction of methoxy substituted sulfamidate **1c** with benzoic acid (**2a**) formed expected product **3c** in moderate yield (52%). However, naphthyl sulfamidate (**1d**) did not react effectively giving 1,3,4-oxadiazole **3e** in poor yield. Notably, bromo derivatives of sulfamidate **1e** with benzoic acid (**2a**) did not afford the desired product (**3f**). Nonetheless, when sulfamidate **1c** was reacted with pyridine carboxylic acid **2c**, it formed the expected product with inseparable isomer in poor yield. Further, 4-hydroxybenzoic acid (**2d**) did not react with sulfamidate **1c** to form desire product **3h**. Next, we also sought to study the reactivity of other carboxylic acids with sulfamidates. So, apart from the products shown in **Scheme 3**, we also attempted other reactions to study reactivity of sulfamidate with other carboxylic acids (see supporting information, **Scheme S1**). For example, difluoro arylacetic acid, pyrimidine-2-carboxylic acid, terephthalic acid etc. - did not react well with sulfamidates. This observation intrigued us to study the reactivity of acyclic *N*-sulfonylimines with carboxylic acids after successful model reaction shown in **Scheme 2**.

As shown in **Scheme 4**, acyclic *N*-sulfonylimine substrates were reacted with benzoic acids. Unlike halogenated sulfamidates, the reaction of halogenated acyclic *N*-sulfonylimine **4b** reacted well with benzoic acid (**2a**) and 4-bromo-2-methyl benzoic acid (**2b**), giving desired products **5b** and **5c** in 53% and 37% yields, respectively. Further, the synthesis of **5d** and **5e** were achieved successfully using trimethoxy substituted *N*-sulfonylimine (**4c**), and 4-hydroxy 3-nitro substituted *N*-sulfonylimine (**4e**), and they were well tolerated to afford desired products **5d** and **5e** (70% and 64% yields, respectively).

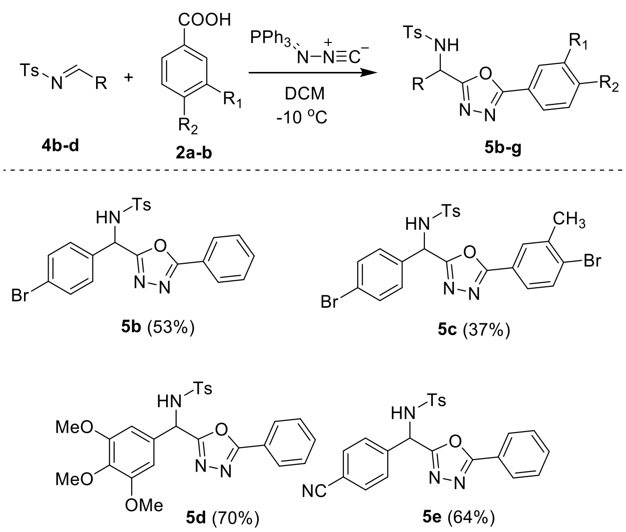

Scheme 4. Substrate scope for acyclic *N*-sulfonylimine with carboxylic acids used as training data.

2.4. Decision tree based chemical reactivity flowcharts

Considering heterogeneous reactivity of cyclic and acyclic sulfonylimines, motivated us to develop a machine learning model using the successful and unsuccessful reactions. We trained decision tree[45] models using the Extended Connectivity Fingerprints[46] of carboxylic acid and imine (**Figure 4**). We used bootstrapping of several decision tree models to ensure robustness of our model for predicting prospective experimental outcomes (see **Supporting text for bootstrapping of the decision tree models** for details). A Cohen Kappa statistic of 0.706 was obtained, suggesting strong inter-model reliability on limited training data (20 reactions).[47,48] All decisions made by the ML model were highly confident except for the final decision (green box in Figure 4). This decision is only supported by a single reaction and that reaction is identified by either *p*-toluic acid or an amine substitution. Therefore, the model is unable to distinguish between specific features that resulted in a successful reaction. To elucidate chemistry at this step, we tested the reaction between **1c** (imine without an amine substitution) and **2b** (*p*-toluic acid) and

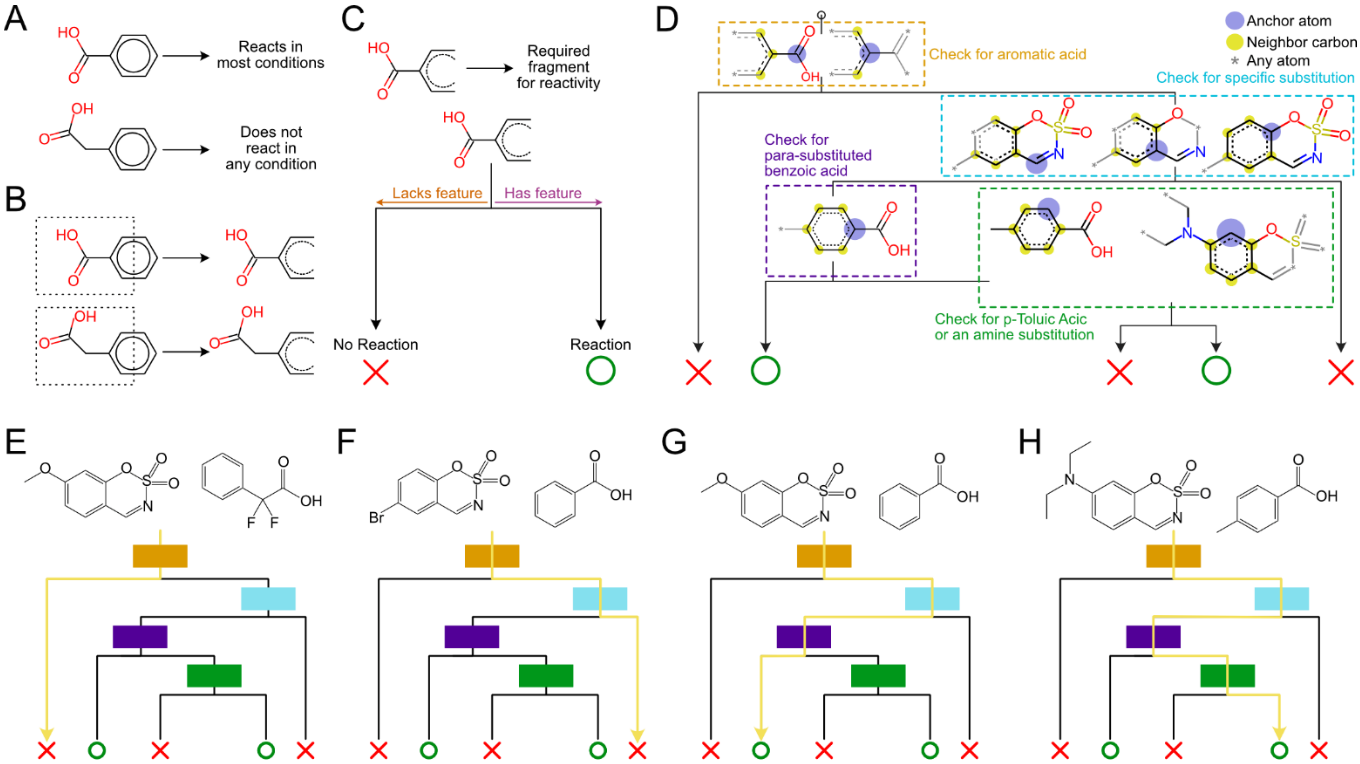

Figure 4. Chemical reactivity flowchart. Decision tree based chemical model for the substrate scope of the reaction between the imine and acid. **A-C**. Showing a pictorial explanation of how the model assigns rules for predicting reactivity**. D.** Showing the final bootstrapped model trained on all data with details for each rule shown in colored boxes. **E-H.** Examples of each of these rules using the training data. Box colors represents features shown in **D** and yellow line of the flowchart shows the outcome of the reaction based on chemical features.

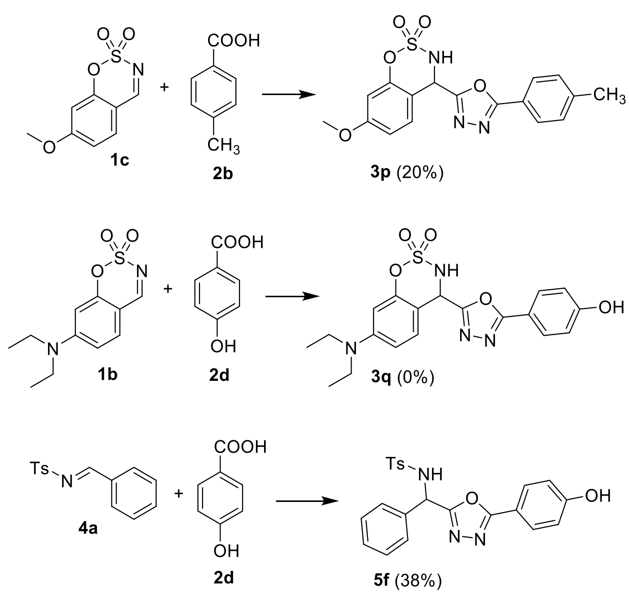

Scheme 5. Reactions performed to test the ML model

noted that the reaction occurred. Conversely, the reaction between **1b** (imine with an amine substitution) and **2d** (4-hydroxy benzoic acid) did not occur. These results show that the final decision should check for *p*-toluic acid and not an amine substitution. Finally, we tested **2d** with the acyclic imine **4a** to see if this rule applied to acyclic amines and noted that the reaction does occur. These reactions are shown in **Scheme 5** and show how our ML strategy can be used to better understand and expand the substrate scope of an MCR.

CONCLUSIONS

In summary, we have developed a fast MCR of acyclic or cyclic *N*-sulfonylimines that was used as a representative reaction type to develop ML models for predicting reaction outcomes in a blind prospective manner. The fast and peculiar reactivity mechanism of *N*-sulfonylimines was explained using DFT calculation to understand the critical role of transition states and intermediates. Bootstrapped decision tree-based ML models resulted in a chemical reactivity flowchart that explained the choices made by the model to predict reaction outcomes. The human interpretable ML approach can be extended to explore any MCR or any chemical reaction used to synthesize a library of compounds in a quick and efficient manner. This work provides a framework for developing fast MCRs, understanding the underlying reaction mechanism and identifying chemical features for predicting the reactivity of components that results in successful reactions to save valuable time for chemists to not chase dead-end leads.

ASSOCIATED CONTENT

Supporting Information

The Supporting Information is available free of charge on the ACS Publications website. Copies of ^{1}H and ^{13}C NMR spectra for all new compounds, additional discussion of the suggested mechanism, and the validation of the machine learning model are included in this document.

AUTHOR INFORMATION

Corresponding Author

Correspondence: gchopra@purdue.edu; Tel.: +1-765-496-6108

Present Addresses

Purdue Institute of Drug Discovery, 720 Clinic Drive, West Lafayette 47906, IN, USA.

Author Contributions

‡These authors contributed equally.

Notes

The authors declare no competing financial interests.

ACKNOWLEDGMENT

This work was supported in part by a Purdue University start-up package from the Department of Chemistry at Purdue University, Ralph W. and Grace M. Showalter Research Trust award, the Integrative Data Science Initiative award, the Jim and Diann Robbers Cancer Research Grant for New Investigators award and NIH NCATS ASPIRE Design Challenge awards to Gaurav Chopra and a Lynn Fellowship to Jonathan Fine. Additional support, in part by, a NCATS Clinical and Translational Sciences Award from the Indiana Clinical and Translational Sciences Institute (UL1TR002529), and the Purdue University Center for Cancer Research NIH grant P30 CA023168 are also acknowledged. The content is solely the responsibility of the authors and does not necessarily represent the official views of the National Institutes of Health.

REFERENCES

(1) Corey, E. J.; Wipke, W. T. Computer-Assisted Design of Complex Organic Syntheses Published by : American Association for the Advancement of Science Stable URL : Http://Www.Jstor.Org/Stable/1727162 Digitize , Preserve and Extend Access to Science of New Computer-Assisted Design of C. *Science (80-.).* **1969**, *166* (3902), 178–192.

(2) Gao, H.; Struble, T. J.; Coley, C. W.; Wang, Y.; Green, W. H.; Jensen, K. F. Using Machine Learning to Predict Suitable Conditions for Organic Reactions. *ACS Cent. Sci.* **2018**, *4* (11), 1465–1476.

(3) Granda, J. M.; Donina, L.; Dragone, V.; Long, D. L.; Cronin, L. Controlling an Organic Synthesis Robot with Machine Learning to Search for New Reactivity. *Nature* **2018**, *559* (7714), 377–381.

(4) Lavecchia, A. Machine-Learning Approaches in Drug Discovery: Methods and Applications. *Drug Discov. Today* **2015**, *20* (3), 318–331.

(5) Rodríguez-Pérez, R.; Miyao, T.; Jasial, S.; Vogt, M.; Bajorath, J. Prediction of Compound Profiling Matrices Using Machine Learning. *ACS Omega* **2018**, *3* (4), 4713–4723.

(6) Ma, J.; Sheridan, R. P.; Liaw, A.; Dahl, G. E.; Svetnik, V. Deep Neural Nets as a Method for Quantitative Structure-Activity Relationships. *J. Chem. Inf. Model.* **2015**, *55* (2), 263–274.

(7) Fooshee, D.; Mood, A.; Gutman, E.; Tavakoli, M.; Urban, G.; Liu, F.; Huynh, N.; Van Vranken, D.; Baldi, P. Deep Learning for Chemical Reaction Prediction. *Mol. Syst. Des. Eng.* **2018**, *3* (3), 442–452.

(8) Segler, M. H. S.; Waller, M. P. Neural-Symbolic Machine Learning for Retrosynthesis and Reaction Prediction. *Chem. - A Eur. J.* **2017**.

(9) Coley, C. W.; Green, W. H.; Jensen, K. F. Machine Learning in Computer-Aided Synthesis Planning. *Acc. Chem. Res.* **2018**, *51* (5).

(10) Ahneman, D. T.; Estrada, J. G.; Lin, S.; Dreher, S. D.; Doyle, A. G. Predicting Reaction Performance in C–N Cross-Coupling Using Machine Learning. *Science (80-.).* **2018**, *360* (6385), 186–190.

(11) Nielsen, M. K.; Ahneman, D. T.; Riera, O.; Doyle, A. G. Deoxyfluorination with Sulfonyl Fluorides: Navigating Reaction Space with Machine Learning. *J. Am. Chem. Soc.* **2018**, *140* (15), 5004–5008.

(12) Miyabe, H.; Ueda, M.; Naito, T. N-Sulfonylimines as an Excellent Acceptor for Intermolecular Radical Reactions. *Chem. Commun.* **2000**, No. 20, 2059–2060.

(13) Izquierdo, J.; Pericàs, M. A. A Recyclable, Immobilized Analogue of Benzotetramisole for Catalytic Enantioselective Domino Michael Addition/Cyclization Reactions in Batch and Flow. *ACS Catal.* **2016**, *6* (1), 348–356.

(14) Stubbing, L. A.; Savage, G. P.; Brimble, M. A. N-Alkylsulfonylimines as Dipolarophiles in Cycloaddition Reactions. *Chemistry - An Asian Journal*. January 2013, pp 42–48.

(15) Luo, Y.; Hepburn, H. B.; Chotsaeng, N.; Lam, H. W. Enantioselective Rhodium-Catalyzed Nucleophilic Allylation of Cyclic Imines with Allylboron Reagents. *Angew. Chemie - Int. Ed.* **2012**, *51* (33), 8309–8313.

(16) Xiong, X. F.; Zhang, H.; Peng, J.; Chen, Y. C. Direct Asymmetric Michael Addition of Cyclic N-Sulfonylimines to α,β-Unsaturated Aldehydes. *Chem. - A Eur. J.* **2011**, *17* (8), 2358–2360.

(17) Laha, J. K.; Jethava, K. P. Access to Imidazolidine-Fused Sulfamidates and Sulfamides Bearing a Quaternary Center via 1,3-Dipolar Cycloaddition of Nonstabilized Azomethine Ylides. *J. Org. Chem.* **2017**, *82* (7), 3597–3604.

(18) Laha, J. K.; Jethava, K. P.; Tummalapalli, K. S. S.; Sharma, S. Synthesis of Mono-N-Sulfonylimidazolidines by a 1,3-Dipolar Cycloaddition Strategy, as an Alternative to Selective N-Sulfonylation, and Their Ring Cleavage To Afford 1,2-Diamines. *European J. Org. Chem.* **2017**, *2017* (31), 4617–4624.

(19) Hu, P.; Hu, J.; Jiao, J.; Tong, X. Amine-Promoted Asymmetric (4+2) Annulations for the Enantioselective Synthesis of Tetrahydropyridines: A Traceless and Recoverable Auxiliary

Strategy. *Angew. Chemie - Int. Ed.* **2013**, *52* (20), 5319–5322.
(20) Kravina, A. G.; Mahatthananchai, J.; Bode, J. W. Enantioselective, NHC-Catalyzed Annulations of Trisubstituted Enals and Cyclic n-Sulfonylimines via α,β-Unsaturated Acyl Azoliums. *Angew. Chemie - Int. Ed.* **2012**, *51* (37), 9433–9436.
(21) Chen, X. Y.; Lin, R. C.; Ye, S. Catalytic [2+2] and [3+2] Cycloaddition Reactions of Allenoates with Cyclic Ketimines. *Chem. Commun.* **2012**, *48* (9), 1317–1319.
(22) Spielmann, K.; Lee, A. Van Der; De Figueiredo, R. M.; Campagne, J. M. Diastereoselective Palladium-Catalyzed (3 + 2)-Cycloadditions from Cyclic Imines and Vinyl Aziridines. *Org. Lett.* **2018**, *20* (5), 1444–1447.
(23) Nishimura, T.; Noishiki, A.; Chit Tsui, G.; Hayashi, T. Asymmetric Synthesis of (Triaryl)Methylamines by Rhodium-Catalyzed Addition of Arylboroxines to Cyclic N-Sulfonyl Ketimines. *J. Am. Chem. Soc.* **2012**, *134* (11), 5056–5059.
(24) Wang, H.; Jiang, T.; Xu, M. H. Simple Branched Sulfur-Olefins as Chiral Ligands for Rh-Catalyzed Asymmetric Arylation of Cyclic Ketimines: Highly Enantioselective Construction of Tetrasubstituted Carbon Stereocenters. *J. Am. Chem. Soc.* **2013**, *135* (3), 971–974.
(25) Li, Y.; Yu, Y. N.; Xu, M. H. Simple Open-Chain Phosphite-Olefin as Ligand for Rh-Catalyzed Asymmetric Arylation of Cyclic Ketimines: Enantioselective Access to Gem-Diaryl α-Amino Acid Derivatives. *ACS Catal.* **2016**, *6* (2), 661–665.
(26) De Munck, L.; Monleón, A.; Vila, C.; Pedro, J. R. Diarylprolinol as a Ligand for Enantioselective Alkynylation of Cyclic Imines. *Adv. Synth. Catal.* **2017**, *359* (9), 1582–1587.
(27) Huang, Y.; Huang, R. Z.; Zhao, Y. Cobalt-Catalyzed Enantioselective Vinylation of Activated Ketones and Imines. *J. Am. Chem. Soc.* **2016**, *138* (20), 6571–6576.
(28) Quan, M.; Wang, X.; Wu, L.; Gridnev, I. D.; Yang, G.; Zhang, W. Ni(II)-Catalyzed Asymmetric Alkenylations of Ketimines. *Nat. Commun.* **2018**, *9* (1), 1–11.
(29) Khalilullah, H.; J. Ahsan, M.; Hedaitullah, M.; Khan, S.; Ahmed, B. 1,3,4-Oxadiazole: A Biologically Active Scaffold. *Mini-Reviews Med. Chem.* **2012**, *12* (8), 789–801.
(30) Verma, G.; Khan, M. F.; Akhtar, W.; Alam, M. M.; Akhter, M.; Shaquiquzzaman, M. A Review Exploring Therapeutic Worth of 1,3,4-Oxadiazole Tailored Compounds. *Mini-Reviews Med. Chem.* **2019**, *19* (6), 477–509.
(31) Katritzky, A. R.; Rees, C. W. *Comprehensive Heterocyclic Chemistry*; Elsevier, 2009; Vol. 1–7.
(32) Zhang, H. Z.; Zhao, Z. L.; Zhou, C. H. Recent Advance in Oxazole-Based Medicinal Chemistry. *European Journal of Medicinal Chemistry*. 2018, pp 444–492.
(33) Patel, K. D.; Prajapati, S. M.; Panchal, S. N.; Patel, H. D. Review of Synthesis of 1,3,4-Oxadiazole Derivatives. *Synth. Commun.* **2014**, *44* (13), 1859–1875.
(34) Huck, B. R.; Kötzner, L.; Urbahns, K. Small Molecules Drive Big Improvements in Immuno-Oncology Therapies. *Angewandte Chemie - International Edition*. Wiley-VCH Verlag April 2018, pp 4412–4428.
(35) Chang, D. J.; Jeong, M. Y.; Song, J.; Jin, C. Y.; Suh, Y. G.; Kim, H. J.; Min, K. H. Discovery of Small Molecules That Enhance Astrocyte Differentiation in Rat Fetal Neural Stem Cells. *Bioorganic Med. Chem. Lett.* **2011**.
(36) Slobbe, P.; Ruijter, E.; Orru, R. V. A. Recent Applications of Multicomponent Reactions in Medicinal Chemistry. *MedChemComm*. Royal Society of Chemistry September 2012, pp 1189–1218.
(37) Rotstein, B. H.; Zaretsky, S.; Rai, V.; Yudin, A. K. Small Heterocycles in Multicomponent Reactions. *Chemical Reviews*. American Chemical Society 2014, pp 8323–8359.
(38) Dömling, A.; Wang, W.; Wang, K. Chemistry and Biology of Multicomponent Reactions. *Chemical Reviews*. June 2012, pp 3083–3135.
(39) Saiz, C.; Wipf, P.; Manta, E.; Mahler, G. Reversible Thiazolidine Exchange: A New Reaction Suitable

for Dynamic Combinatorial Chemistry. *Org. Lett.* **2009**, *11* (15), 3170–3173.

(40) Maskrey, T. S.; Frischling, M. C.; Rice, M. L.; Wipf, P. A Five-Component Biginelli-Diels-Alder Cascade Reaction. *Front. Chem.* **2018**, *6* (AUG), 376.

(41) Ramazani, A.; Rezaei, A. Novel One-Pot, Four-Component Condensation Reaction: An Efficient Approach for the Synthesis of 2,5-Disubstituted 1,3,4-Oxadiazole Derivatives by a Ugi-4CR/Aza-Wittig Sequence. *Org. Lett.* **2010**, *12* (12), 2852–2855.

(42) Appavoo, S. D.; Kaji, T.; Frost, J. R.; Scully, C. C. G.; Yudin, A. K. Development of Endocyclic Control Elements for Peptide Macrocycles. *J. Am. Chem. Soc.* **2018**, *140* (28), 8763–8770.

(43) Frost, J. R.; Scully, C. C. G.; Yudin, A. K. Oxadiazole Grafts in Peptide Macrocycles. *Nat. Chem.* **2016**, *8* (12), 1105–1111.

(44) Contreras, R. R.; Fuentealba, P.; Galván, M.; Pérez, P. A Direct Evaluation of Regional Fukui Functions in Molecules. *Chem. Phys. Lett.* **1999**, *304* (5–6), 405–413.

(45) Quinlan, J. R. Induction of Decision Trees. *Mach. Learn.* **1986**, *1* (1), 81–106.

(46) Rogers, D.; Hahn, M. Extended-Connectivity Fingerprints. *J. Chem. Inf. Model.* **2010**, *50* (5), 742–754.

(47) Cohen, J. Weighted Kappa: Nominal Scale Agreement Provision for Scaled Disagreement or Partial Credit. *Psychol. Bull.* **1968**, *70* (4), 213–220.

(48) McHugh, M. L. Interrater Reliability: The Kappa Statistic. *Biochem. Medica* **2012**, *22* (3), 276–282.

For Table of Contents Only